Materials Horizons

ROYAL SOCIETY OF CHEMISTRY

COMMUNICATION

View Article Online
View Journal | View Issue

Cite this: *Mater. Horiz.*, 2025, **12**, 9601

Received 3rd June 2025,
Accepted 30th July 2025

DOI: 10.1039/d5mh01044f

rsc.li/materials-horizons

Ion exchange selectivity governs phase selection in zeolite synthesis

Anjul Rais, †[a] Dries Vandenabeele, †[a] Nikolaus Doppelhammer, [a] Karel Asselman, [a] Wauter Wangermez,[a] Christine E. A. Kirschhock [a] and Eric Breynaert *[ab]

Building on insights obtained in homo-ionic zeolite syntheses with alkali cations, phase selection in mixed systems was investigated using hydrated silicate ionic liquid-based media. This study relates phase selection and framework composition to ion exchange selectivity in zeolites. The analysis confirms and extends phase selection heuristics previously obtained in single-cation studies and enables targeted zeolite synthesis in multiple cation systems.

New concepts

Even though zeolites are porous materials, they crystallize as a dense phase consisting of a silicate network embedding pore filling species that template the growing solid. Focusing on inorganically templated zeolites, phase selection can be rationalised based on cation framework interactions. Overall, the framework with the highest fractional cation occupancy will emerge as it maximizes favourable cation-framework interactions. But which cation dominates zeolite formation in syntheses containing cation mixtures? Comparing phase selection in mixed alkali cation syntheses with the cation exchange selectivity of zeolites, reveals these phase selection and cation exchange are linked. This new concept allows to predict phase selection in complex inorganic zeolite syntheses based on the cation exchange selectivity coefficients of typically observed aluminosilicate zeolites, intrinsically linking the selectivity of the final framework with the cation exchange selectivity of the negatively charged silicate oligomers present in the synthesis liquid.

Introduction

Even though zeolites are usually perceived as porous materials, they crystallize as dense solids.[1] In as synthesised state, the pores and channels are occupied by a combination of charge balancing species and water. During zeolite genesis, these extra-framework species self-organise to optimally interact with the framework and with each other. To make the intrinsic porosity of the zeolite topology accessible, post synthetic treatments such as drying, calcination and cation exchange are commonly applied. Applied separately or in combination, these treatments serve to functionalise or activate the material.[2–8]

Using homo-ionic systems, it was recently shown that phase selection in as made inorganic zeolites optimizes framework-cation interactions by establishing a maximal (fractional) cation occupancy of the framework.[9] Phase selection in mixed cation systems however still awaits complete rationalisation. In such systems, ion exchange phenomena play a vital role.

Zeolites are built up from cation–anionic silicate oligomer assemblies.[10–14] As these cations are not part of the covalent framework but only electrostatically interact with said framework, they can be exchanged. In the same way, it is possible to describe liquid anionic aluminosilicate oligomers as ion exchangers. It stands to reason that the affinity of a specific cation for a distinct chemical environment – the cation exchange selectivity – has a decisive influence on their speciation in the synthesis liquid and thus also on phase selection. This suggests a link between phase selection and cation exchange selectivity of zeolite materials.

Overall, alkali cation exchange in zeolites follows the selectivity sequence: $Cs^+ > K^+ > Na^+ > Li^+$, aligning with the empiric lyotropic series.[15–18] The cation exchange selectivity series also applies to other (alumino-)silicate materials such as clays and phyllosilicates.[19] Maes and Cremers first correlated the energy of hydration of different monovalent cations to their cation exchange selectivity coefficient in clays and zeolites, identifying the decreasing Gibbs energy of the overall system as the thermodynamic driving force.[20,21]

While most zeolitic materials exhibit an ion exchange selectivity series conforming to the lyotropic series, each material exhibits specific selectivity constants (K_C) for a given cation. These can be largely different and vary with site geometry, hydration and the occupancy of distinct cation exchange sites (Table 1).[22–24] The ion exchange process replacing an adsorbed cation A^+ by a dissolved cation B^+ can be represented as:

$$\text{Zeolite} - A^+ + B^+_{(aq)} \rightleftharpoons \text{Zeolite} - B^+ + A^+_{(aq)}$$

[a] *Centre for Surface Chemistry and Catalysis Characterisation and Application Team (COK-KAT), KU Leuven, Leuven 3001, Belgium. E-mail: eric.breynaert@kuleuven.be*

[b] *NMRCoRe-NMR/X-Ray platform for Convergence Research, KU Leuven, Leuven 3001, Belgium*

† These authors contributed equally.

Table 1 Ln KC Values for zeolites with varying Si/Al ratios and exchanged cations

Zeolite type	Si/Al	Cation exchanged	Ln (K_C)	Ref.
FAU	1.37	$Na^+ \rightarrow Cs^+$	1.22	26
MFI	12.3	$Na^+ \rightarrow Cs^+$	3.92	26
YFI	11.1	$Na^+ \rightarrow Cs^+$	4.29	26
MOR	9.88	$Na^+ \rightarrow Cs^+$	5.17	26
MOR	8.37	$Na^+ \rightarrow Cs^+$	5.23	26
LTA	1.12	$Na^+ \rightarrow Cs^+$	3.01	26
HEU (natural)	—	$Na^+ \rightarrow Cs^+$	5–4.95	29
		$K^+ \rightarrow Cs^+$	2.67–2.74	29
CHA (Natural)	~4.5	$Na^+ \rightarrow Cs^+$	4.72–4.70	29
		$K^+ \rightarrow Cs^+$	2.12–2.18	29
CHA	2.0	$Na^+ \rightarrow Cs^+$	4.55–4.45	29
		$K^+ \rightarrow Cs^+$	3.10–3.11	29
MOR	5.0	$Na^+ \rightarrow Cs^+$	6.17–5.96	29
Stilbite (STI)	~2.7	$Na^+ \rightarrow Cs^+$	1.95	30
		$K^+ \rightarrow Cs^+$	1.24	30
Clinoptilolite (HEU)	~5.0	$Na^+ \rightarrow Cs^+$	2.96	31
PHI	3.93	$Na^+ \rightarrow Cs^+$	2.82	32
PHI (Natural)	2.0	$Na^+ \rightarrow Cs^+$	3.27	33

The selectivity of the framework for B^+ as compared to A^+ can therefore be expressed quantitatively using the corrected selectivity coefficient K_C. According to the Gaines and Thomas formalism,[25] K_C is defined as:

$$ {}^{A}_{B}K_C = \frac{N_A^{Z_B} \cdot a_B^{Z_A}}{N_B^{Z_A} \cdot a_A^{Z_B}} $$

with 'N' denoting the equivalent ionic fractions of species A and B on the zeolite, and 'a' their respective activities in solution, and where Z_A and Z_B are the charges of ions A and B, respectively. K_C values express how well the cation exchange sites in the framework satisfy the coordination preferences of specific cations. Na^+, for example, is a cation with a high charge density and low polarizability, and thus has a high hydration energy. It therefore favours environments where water molecules can take part in its coordination sphere, and adsorption sites that exhibit low polarizability.[26] Cs^+, in contrast, exhibits a much larger ionic radius and low energy of hydration, presenting a cationic species with low charge density and high polarizability.[26] It therefore prefers cation exchange sites where it can coordinate as many framework oxygens as possible, avoiding water as coordination partner.[27] In ABW for instance, Cs^+ is surrounded by 10 framework oxygens and no water.[9] In pollucite (ANA topology), its coordination even increases to 12.[28] K^+ presents an in-between case. Examples of exchange selectivity coefficients of specific materials for specific cations are given in Table 2.

Of course, exceptions exist where exchange selectivities deviate from the typical selectivity series. In hydroxysodalite, for example, the series is almost fully reversed ($Na^+ > Li^+ > K^+ > Rb^+ > Cs^+$).[15] Recent work showed how the hydroxysodalite structure is templated by a supramolecular ion $[Na_4(H_3O_2)]^{3+}$, related to a high selectivity of aluminosilicate oligomers in the synthesis liquid for these ions.[49] Hydroxysodalite {ideally $Na_8(OH)_2[Al_6Si_6O_{24}](H_2O)_4$}, hosting $[Na_4(H_3O_2)]^{3+}$ ions in the sod cage, exhibits the most negative enthalpy of formation.[50] In general the selectivity of hydroxysodalite for Na^+ ions derives from its selectivity for the $[Na_4(H_3O_2)]^{3+}$ supramolecular complex. These show a lower charge, spread over a larger volume, exhibiting a lower charge density. As a result the sodalite cage forms, to perfectly accommodate the super-ion.

The present study investigates the competition between different alkali cations (Na^+, K^+ and Cs^+) as templates for zeolites. To avoid local and kinetic effects, often occurring in gel syntheses, all synthesis experiments started from Al-doped Hydrated Silicate Ionic Liquids (HSILs; Si/Al = 16.67, more info. in SI).[51–53] Overall, it was found that large cations with low charge density and low enthalpy of hydration typically dominate phase selection. Polarizable cations have been shown to associate more strongly with aluminosilicate oligomers compared to hydroxide or water molecules in the synthesis mixture.[10,54]

Results and discussion

Synthesis compositions studied had the following composition: 0.5 $Si(OH)_4$–0.03$Al(OH)_3$–xMOH–$y$$H_2O$ with batch alkalinity (SiO_2/OH^-) ranging from 0.125 to 1 and H_2O/MOH from 4 to 100. These ranges compare to the synthesis window of previous studies investigating phase selection in homo-ionic systems with alkali ions.[9,55] The Na : K : Cs cation ratios were set to 1 : 1 : 1, 9 : 9 : 2, and 1 : 1 : 0 respectively. Solid products were

Table 2 Selectivity series of monovalent cations in aluminosilicate frameworks and related materials

Material type	Selectivity series (for monovalent metals)	Ref.
Sodalite (SOD)	$Na^+ > Li^+ > K^+ > Rb^+ > Cs^+$	15
Zeolite A (LTA)	$Na^+ > K^+ > Li^+ > Cs^+$	16
Zeolite X/Y (FAU)	$Ag^+ \gg Cs^+ > Rb^+ > K^+ > Na^+ > Li^+$	16, 34, 35
Chabazite (CHA)	$Cs^+ > Rb^+ > K^+ > Na^+ > Li^+$	16, 35, 36
Merlinoite (MER)	$K^+ > Na^+ > Cs^+$	16, 37, 38
Clinoptilolite (HEU)	$Cs^+ > Rb^+ > K^+ > Na^+ > Li^+$	16, 39
Analcime (ANA)	$Na^+ > K^+ > Ag^+ > Li^+$	40, 41
Edingtonite (EDI)	$Cs^+ > K^+ > Na^+ > Li^+$	16
Erionite (ERI)	$Rb^+ > Cs^+ > K^+ > Na^+ > Li^+$	16, 42, 43
Gismondine (GIS)	$Na^+ > K^+ > Li^+ > Cs^+$	16, 44
ZSM-5 (MFI)	$Cs^+ > Rb^+ > K^+ > Na^+ > Li^+$	16, 45
Phillipsite (PHI)	$Cs^+ > Rb^+ > K^+ > Na^+ > Li^+$	16, 46
Montmorillonite (clay)	$Cs^+ > Rb^+ > K^+ > Na^+ > Li^+$	47
Vermiculite (clay)	$Cs^+ > Rb^+ > K^+ > Na^+ > Li^+$	19, 47
Muscovite mica	$Cs^+ > K^+ > Rb^+ \gg Na^+ > Li^+$	48

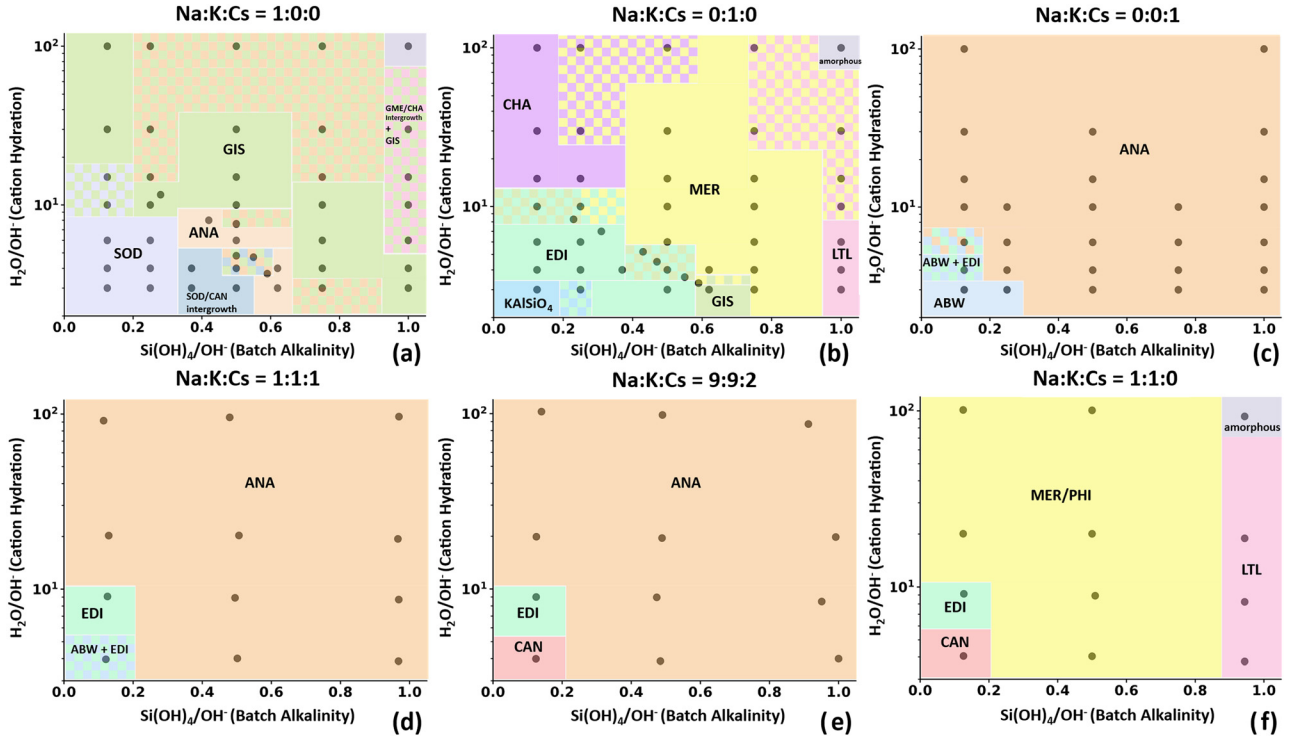

Fig. 1 Frameworks observed in all composition ranges for sodium–potassium–cesium mixed system comparing with (a) pure Cs (b) pure K (c) pure Na with (d) Na : K : Cs = 1 : 1 : 1, (e) Na : K : Cs = 9 : 9 : 2 (f) Na : K : Cs = 1 : 1 : 0.

recovered after one week of synthesis at 90 °C in a rotary oven. Following rinsing with pure water and drying at 70 °C, the phases were identified using PXRD (Fig. S7–S9). The framework types are shown in Fig. 1(d)–(f) and compared with corresponding homo-ionic syntheses in identical synthesis conditions (Fig. 1(a)–(c)).[55]

General trend

Interestingly, phase selection in the equimolar mixed cation syntheses (1 : 1 : 1) yielded 3 distinct topologies ANA, ABW and EDI, exhibiting a strong correlation with pure Cs^+ systems. Deviations from topologies obtained in pure Cs^+ systems were observed only under highly alkaline conditions ($SiO_2/OH^- < 0.25$) and reduced water content ($H_2O/OH^- < 6$) where EDI and ABW-EDI phase mixes occur. Also, the Si/Al ratio of the frameworks remained highly similar to the homo-ionic system[55–57] The phase boundary between the ANA topology and the other frameworks (Si/Al = 1.8) did not change, nor did the crystal morphology (Fig. S1). Pollucite, the Cs variant of the ANA topology, typically crystallizes in spherical crystals, here ranging from 35–60 nm. Analysis of the cation composition of the product revealed that about 95% of the incorporated cations are Cs-ions (Table A3, SI). The close similarity between the phase boundaries of the homo-ionic Cs^+ system and the Cs^+-containing mixed cation systems is therefore not surprising (Fig. S2).

The dominant influence of Cs^+ on phase selection can be explained by considering the aluminosilicate oligomers in the synthesis mixture as liquid cation exchangers with a similar selectivity series and comparable selectivity coefficients compared to the frameworks formed. As the synthesis liquids are overall charge-neutral, similar to solid aluminosilicates, the liquid (alumino-)silicates oligomers require cation association to balance their negative charge. Negative charges arise from the combination of silicate deprotonation and isomorphic substitution of Si^{4+} by Al^{3+}. As ion associations govern the structuring role of inorganic cations during zeolite formation, a link between the ion-exchange selectivity of oligomers with phase selection is to be expected.[10–13]

Traditional concepts, such as Bjerrum's model,[58] suggest that smaller cations with high charge density such as Na^+ should form stronger ion-pairs compared to larger cations such as Cs^+. The present synthesis results however suggest the opposite, indicating Cs^+ to more efficiently stabilize local environments that favour aluminosilicate condensation.[10] The results are in line with data from McCormick *et al.* who also reported Cs^+-ions to have a larger affinity for silicates than Na^+, owing to their ability to interact with (larger) silicate anions with more delocalised charge. The experimental data also is in line with recent simulations by Vekeman *et al.* on hydrated silicate ionic liquids (HSILs).[54] The simulations demonstrate that, in contrast to Na^+ which typically exhibits a localized, directional coordination with deprotonated silanol oxygens and water, Cs^+ coordinates with deprotonated, as well as regular silanols, avoiding water.[54] Even though for technical reasons, the simulations were limited to silicate monomers, the results imply that Cs^+ would better catalyse oligomer condensation due to its capacity to bridge multiple aluminosilicate species.[9] The high affinity of Cs^+ for polarizable local environments in liquid silicate oligomers is in

full agreement with its low enthalpy of hydration, compared to Na^+ and K^+.

In the mixed systems (Na : K : Cs = 1 : 1 : 1) only typical Cs-zeolites are found.[9,59] The final materials nearly exclusively contain Cs cations (Table A3, SI), supporting the hypothesis that cation coordination to (alumino-)silicates governs phase selection in mixed cation systems. The following sections address two validation experiments that underpin this hypothesis.

The fact that cation exchange selectivity constants for Cs^+ are typically very high as compared to those for K^+ and Na^+ is roughly independent on the type of material (Table 2), implying that even very low equivalent fractions of Cs^+ dominate exchange equilibria. Therefore, Cs should still dominate phase selection at much lower concentrations compared to sodium and potassium. Under synthesis conditions identical to those used for equimolar system, the cesium content was reduced to reach a Na : K : Cs ratio of 9 : 9 : 2. The resulting zeolite topologies closely resemble those obtained in the homoionic Cs^+ system (Fig. 1(c) and (e)). The synthesized pollucite predominantly incorporated Cs^+ ($\sim$90%) and exhibited a Si/Al ratio consistent with that of the zeolites formed in the homo-ionic Cs^+ system (Table A3, SI). At high total cation concentrations and alkalinity, however a CAN phase is obtained, which will be addressed later.

The second validation is found in the binary sodium – potassium system, where the proposed hypothesis implies that K-stabilized and -filled zeolites are expected to form. Their lower charge density (and lower enthalpy of hydration) relative to Na^+, should result in a stronger affinity for coordination with aluminosilicates, enhancing the structure-directing role of K^+ compared to Na^+. Consistent with these expectations, syntheses conducted with a cation ratio of 1 : 1 : 0 (Na : K : Cs) resulted in the formation of typical K-stabilized zeolites such as EDI, GIS, MER, CHA, and LTL.[60–62] Exceptions are again encountered in the highly alkaline regime, where the cations have a synergetic effect on framework formation (Fig. 1(f)). These will also be addressed in the next section.

The phase selection observed in the present study are also in line with recent observations in gel syntheses. Mallette and coworkers investigated zeolite crystallisation in a series of binary and ternary systems with inorganic cations.[63] Targeting the synthesis of CHA, they combined K^+ with other (earth)alkali cations. In line with our observations, the Cs-containing mixtures (going as low as 10%) always yielded pollucite. In combination with K^+ (K : Cs = 9 : 1), the synthesis however yielded a chabazite/pollucite mixture. Whereas in systems with a Cs/Al $\geq$ 1 only pollucite would be formed, the low Cs/Al ration in the reported syntheses most likely also allowed CHA formation by consuming the excess aluminium after Cs is depleted. As would be expected, Mallette *et al.* also formed the typical K-CHA in K^+ based syntheses containing 10% up to 10% of Na^+ and/or Li^+. In line with the synthesis results of the present paper, in Cs^+ as well as in K based syntheses, the phase determining cation occupied over 90% of the cation exchange capacity. Ternary syntheses, reported by Ghojavand and Debost, using even lower relative Cs^+ contents (<4% of the cations) only rarely encountered pollucite or other typical Cs-zeolites. Instead, RHO was observed frequently. At such low relative concentrations, Cs^+ can no longer dominate the ion association and thus phase selection in the liquid. Not surprisingly, of all enclosed cations in the products about 30% consisted of Cs.[64,65] Interestingly, higher temperatures (160 °C) were reported to indeed promote the formation of pollucite.[65] Higher synthesis temperatures promote cation aluminosilicate association over cation hydration, thus explaining the formation of the anhydrous pollucite.[1,66]

In their work on interzeolite conversion, Kim *et al.* implemented a mixed cation approach to crystallize CHA instead the GME/CHA intergrowths that typically form in homo-ionic Na-systems. They were able to synthesize pure CHA when adding K, across different alkalinities, in line with the proposed heuristics. They however also found that adding small amounts of other alkali nitrates such as Cs, also worked. Cs/(Cs + Na) ratios up to 17% for example also yielded CHA, which is also a framework exhibiting very high Cs selectivity in ion exchange.[8] Increasing the Cs/Na ratio to 38% yielded ANA. Unfortunately, the authors do not report the cation composition of the solids, hindering a more thorough interpretation of potential synergetic effects.[67]

Ion-synergistic effects

The formation of RHO at very low Cs/Na ratios is a typical example for cation synergy, a concept which is not new. Zeolites such as PHI and RHO only form using specific combinations of respectively Na^+ and K^+ or Na^+ and Cs^+.[68] In the final zeolite, each cation resides in a unique environment tailored to its coordination preference. In RHO, Cs^+ is found in the D8R, coordinating maximally to the framework, while Na^+ resides close to framework oxygens in the large cavity, where it also interacts with water. Pure Cs syntheses, typically yield pollucite with ANA framework, whereas pure Na-systems crystallize phases such as faujasite (FAU) or analcime (ANA).[68]

Also the formation of cancrinite (CAN) at high cation concentrations and high alkalinity can be rationalised by ion synergy. In the homo-ionic Cs^+ and K^+ systems ABW and Kalsilite form respectively, while the mixed Na^+–K^+–Cs^+ system (Na : K : Cs = 9 : 9 : 2 and 1 : 1 : 0) yields CAN. In the binary cation system (Na : K : Cs = 1 : 1 : 0) the final occupancy is $\sim$75% Na^+ and $\sim$25% K^+. In the ternary system, the resulting CAN phase incorporates only traces of K^+, and roughly a Na^+ and Cs^+ ratio of 2 (Table A3, SI). Interestingly, ^{13}C-NMR reports the presence of carbonate in the samples, originating from impurities in the Cs-source (Thermo Scientific; $CsCO_3$ < 5%) or from absorption from the air. Refinement of the Na/Cs CAN shows that Cs^+ closely interacts with the framework in the *can*-cage, while Na^+ is found in the 12-ring channel, interacting with framework and carbonate anions. Similar to hydroxysodalite, CAN is known to readily incorporate anionic species, preferentially carbonate or nitrate, with Na^+ coordinating to framework, water and/or anions. Like in the case of hydroxysodalite, the resulting carbonate-sodium super-ion displays a lower charge density and perfectly fits the topology of CAN.

Updated heuristics for phase selection

For homo-ionic, inorganic systems, Asselman and coworkers derived a set of heuristics that describe why one framework is

favoured over another.[9,66] The present work allows to refine these rules to systems that include multiple competing cations in the liquid:

(i) Framework selection is predominantly governed by maximal fractional cation occupancy for a given Si/Al ratio. This can be modulated by the Gibbs free energy of including water in the framework (enthalpy *vs.* entropy).[1,66,69]

(ii) The Si/Al ratio is determined by synthesis composition and conditions, largely dominated by the water content (activity) and alkalinity.

(iii) Ion exchange selectivity of cations for liquid (alumino-) silicates oligomers, determines the dominant cation(s), which ultimately ''template'' the framework (reflected in its exchange preference). Sometimes resulting in synergetic effects between different cations.

(iv) While the cation composition of the final solid framework will always contain a large fraction of the cation(s) dominating framework selection (rule iii), their final concentration is modulated by the ion exchange selectivity coefficients of all cations for the final framework and their concentration in the liquid at the end of the synthesis.

To describe how these rules interact, we discuss the example of Cs,Na-EDI. In synthesis mixture Na : K : Cs = 1 : 1 : 1 and 9 : 9 : 2, the low water content and high alkalinity of the synthesis liquid dictate a Si/Al ratio of 1.1 (rule iii). Cs has a the highest affinity for liquid aluminosilicates as compared to the other cations in the mix and will therefore dominate the selection of phases that can be formed: in this case ABW, EDI, CAN and ANA (rule iii). In homo-ionic Cs-based media, related systems yield ABW with a trace of EDI, enabling a maximal fractional cation occupancy (rule i). In the mixed Cs : K : Na = 1 : 1 : 1 system, EDI prevails and the final framework contains about 50% Na^+. EDI has two cation sites, one closely following the lyotropic series (Cs > K > Li > Na) and one with a reversed preference (Na > Li > K > Cs), thus explaining the observed cation occupancy.[70] Site 1 has a $\ln(K_C)$ of $\sim$2 (high Cs-preference) and site 2 a $\ln(K_C)$ of ~ -1.5 with a distribution of $\sim$60% for site 1, as reported by ion-exchange experiments.[70] The formation of Na,Cs-EDI over Cs-ABW is explained by the enthalpy of hydration of including water. ABW and EDI have the same number cation positions per T-atom (same fractional occupancy), making cation hydration the determining phase selection parameter. At the same fractions cation occupancy, Cs-ABW has a water/cation ratio of 1, while Na,Cs-EDI exhibits a ratio of 1.25 (rule i).

Conclusions

The present work expands the heuristics of zeolite phase selection in homo-ionic inorganic alkaline conditions to mixed cation systems. Overall, phase selection is governed by the affinity of aluminosilicates for the available cations. Frameworks-cation systems maximize their coulombic interactions by optimising cation coordination. Consequently, the forming topology allows for a maximal fractional cation occupancy. In multi-cation systems (binary and ternary), ion exchange selectivity determines which cations will be integrated into the forming zeolite, thereby co-determining phase selection. The observations directly link ion exchange selectivity coefficients of crystallized aluminosilicate zeolites to those of the negatively charged aluminosilicate oligomers in the synthesis liquid. In this context, zeolite formation resembles common salting-out processes. This implies the ion association between positively charged cations and negatively charged silicate oligomers can be described in a similar way as ion exchange phenomena in which multiple cations compete. In line with typically observations for alkali cation exchange on zeolites, in Cs^+ containing binary and ternary synthesis systems, the selectivity of the cation is high enough to dominate phase selection, even when its fraction in the cation mixture is reduced down to 10%. Speaking in rough terms, this observation can be summarised in the following heuristic: In mixed alkali cation zeolite syntheses, the cation with the highest ion-exchange selectivity, is the best candidate to form a zeolite wherein framework and cations are optimally stabilised.

Author contributions

Investigation: A. R., W. W. and K. A.; formal analysis: A. R., D. V., N. D. and K. A.; writing – original draft: A. R. and D. V.; validation and visualization: A. R., D. V. and E. B.; supervision: N. D., E. B. and C. K.; conceptualization: E. B.; funding acquisition: C. K. and E. B.; review and editing: N. D., K. A., W. W., C. K., and E. B.

Conflicts of interest

There are no conflicts to declare.

Data availability

The data supporting this article have been included as part of the SI. Replication data can be found in Harvard Dataverse: **https://doi.org/10.7910/DVN/H3OLRF**.

Detailed synthesis procedures; Tabulated synthesis compositions; SEM images, powder XRD patterns; elemental analysis of the solid products. See DOI: **https://doi.org/10.1039/d5mh01044f**

Acknowledgements

E. B. and C. K. acknowledge joint funding by the Flemish Science Foundation (FWO; G083318N and G0AC524N) and the Austrian Science Fund (FWF) (funder ID 10.13039/501100002428, grant ID 10.55776/I3680, project ZeoDirect, I3680-N34 and grant ID 10.55776/I6800, project MEmeZe, I6800). This work has received funding from KU Leuven (SIONA, C14/22/099). E. B. acknowledges FWO for a ''Krediet aan navorsers'' 1.5.061.18N. NMRCoRe is supported by the Hercules Foundation (AKUL/13/21), by the Flemish Government as an international research infrastructure (I001321N), and by Department EWI *via* the Hermes Fund

(AH.2016.134). N. D. acknowledges a postdoctoral fellowship from FWO Vlaanderen.

Notes and references

1 D. Vandenabeele, A. Rais, C. Kirschhock and E. Breynaert, *CrystEngComm*, 2025, **27**, 2452–2461.
2 Z. Asgar Pour, Y. A. Alassmy and K. O. Sebakhy, *Crystals*, 2023, **13**, 959.
3 V. Valtchev, G. Majano, S. Mintova and J. Pérez-Ramírez, *Chem. Soc. Rev.*, 2013, **42**, 263–290.
4 E. Pérez-Botella, S. Valencia and F. Rey, *Chem. Rev.*, 2022, **122**, 17647–17695.
5 T. De Baerdemaeker, M. Feyen, T. Vanbergen, U. Müller, B. Yilmaz, F.-S. Xiao, W. Zhang, T. Yokoi, X. Bao, D. E. De Vos and H. Gies, *Chem. Mater.*, 2015, **27**, 316–326.
6 R. Simancas, A. Chokkalingam, S. P. Elangovan, Z. Liu, T. Sano, K. Iyoki, T. Wakihara and T. Okubo, *Chem. Sci.*, 2021, **12**, 7677–7695.
7 E. Eom, M. Song, J.-C. Kim, D. Kwon, D. N. Rainer, K. Gołąbek, S. C. Nam, R. Ryoo, M. Mazur and C. Jo, *JACS Au*, 2022, **2**, 2327–2338.
8 L. Van Tendeloo, W. Wangermez, A. Vandekerkhove, T. Willhammar, S. Bals, A. Maes, J. A. Martens, C. E. A. Kirschhock and E. Breynaert, *Chem. Mater.*, 2017, **29**, 629–638.
9 K. Asselman, D. Vandenabeele, N. Pellens, N. Doppelhammer, C. E. A. Kirschhock and E. Breynaert, *Chem. Mater.*, 2022, **34**, 11081–11092.
10 A. V. McCormick, A. T. Bell and C. J. Radke, *J. Phys. Chem.*, 1989, **93**, 1733–1737.
11 N. Pellens, N. Doppelhammer, S. Radhakrishnan, K. Asselman, C. V. Chandran, D. Vandenabeele, B. Jakoby, J. A. Martens, F. Taulelle, E. K. Reichel, E. Breynaert and C. E. A. Kirschhock, *Chem. Mater.*, 2022, **34**, 7139–7149.
12 A. V. McCormick, A. T. Bell and C. J. Radke, *MRS Proc.*, 1987, **111**, 107.
13 A. V. McCormick, A. T. Bell and C. J. Radke, *J. Phys. Chem.*, 1989, **93**, 1737–1741.
14 D. Vandenabeele, N. Doppelhammer, S. Radhakrishnan, V. Chandran, C. B. Jakoby, C. Kirschhock and E. Breynaert, *Microporous Mesoporous Mater.*, 2024, **374**, 113141.
15 M. Kuronen, R. Harjula, J. Jernström, M. Vestenius and J. Lehto, *Phys. Chem. Chem. Phys.*, 2000, **2**, 2655–2659.
16 A. Dyer, *Studies in Surface Science and Catalysis*, Elsevier, 2007, vol. 168, pp. 525–553.
17 V. Mazzini and V. S. J. Craig, *Curr. Opin. Colloid Interface Sci.*, 2016, **23**, 82–93.
18 J. Lyklema, *Chem. Phys. Lett.*, 2009, **467**, 217–222.
19 B. L. Sawhney, *Clays Clay Miner.*, 1972, **20**, 93–100.
20 A. Maes and A. Cremers, *J. Chem. Soc., Faraday Trans. 1*, 1978, **74**, 1234.
21 B. J. Teppen and D. M. Miller, *Soil Sci. Soc. Am. J.*, 2006, **70**, 31–40.
22 C. Baerlocher, L. B. McCusker, D. Olson and W. M. Meier, Atlas of zeolite framework types, Published on behalf of the Structure Commission of the International Zeolite Association by Elsevier, Amsterdam Boston, 6th rev. edn, 2007.
23 K. Ogawa, M. Nitta and K. Aomura, *J. Phys. Chem.*, 1978, **82**, 1655–1660.
24 W. Baek, S. Ha, S. Hong, S. Kim and Y. Kim, *Microporous Mesoporous Mater.*, 2018, **264**, 159–166.
25 G. L. Gaines and H. C. Thomas, *J. Chem. Phys.*, 1953, **21**, 714–718.
26 N. Katada, H. Tamura, T. Matsuda, Y. Kawatani, Y. Moriwaki, M. Matsuo and R. Kato, *Langmuir*, 2024, **40**, 19324–19331.
27 S. Kwon, C. Kim, E. Han, H. Lee, H. S. Cho and M. Choi, *J. Hazard. Mater.*, 2021, **408**, 124419.
28 K. Asselman, C. Kirschhock and E. Breynaert, *Acc. Chem. Res.*, 2023, **56**, 2391–2402.
29 L. Van Tendeloo, B. De Blochouse, D. Dom, J. Vancluysen, R. Snellings, J. A. Martens, C. E. A. Kirschhock, A. Maes and E. Breynaert, *Environ. Sci. Technol.*, 2015, **49**, 1729–1737.
30 L. L. Ames, *Can. Mineral.*, 1966, **8**, 582–592.
31 D. Moraetis, G. E. Christidis and V. Perdikatsis, *Am. Mineral.*, 2007, **92**, 1714–1730.
32 M. Adabbo, D. Caputo, B. De Gennaro, M. Pansini and C. Colella, *Microporous Mesoporous Mater.*, 1999, **28**, 315–324.
33 L. L. Ames Jr., *Can. Mineral.*, 1965, **8**, 325–333.
34 H. S. Sherry, *J. Phys. Chem.*, 1966, **70**, 1158–1168.
35 R. M. Barrer and D. C. Sammon, *J. Chem. Soc.*, 1955, 2838.
36 R. M. Barrer and J. Klinowski, *J. Chem. Soc., Faraday Trans., 1*, 1972, **68**, 1956.
37 J. D. Sherman, *Adsorption and Ion Exchange Separations*, American Institute of Chemical Engineers, 1978, vol. 74, pp. 98–116.
38 Y. Kakutani, P. Weerachawanasak, Y. Hirata, M. Sano, T. Suzuki and T. Miyake, *RSC Adv.*, 2017, **7**, 30919–30928.
39 S. M. Auerbach, K. A. Carrado and P. K. Dutta, in *Handbook of zeolite science and technology*, ed. M. Dekker, New York, 2003.
40 D. Savage, C. Rochelle, Y. Moore, A. Milodowski, K. Bateman, D. Bailey and M. Mihara, *Mineral. Mag.*, 2001, **65**, 571–587.
41 C. Liu, H. Ma, Y. Qiu and Y. Gao, *Ceram. Int.*, 2019, **45**, 15566–15570.
42 L. L. Ames, *Am. Mineral.*, 1962, **47**, 1317–1326.
43 H. S. Sherry and J. B. Marinsky, Ion Exchange, *A Series of Advances*, Dekker, New York, 1969, vol. 2, pp. 89–133.
44 R. M. Barrer and B. M. Munday, *J. Chem. Soc. A*, 1971, 2909.
45 *Advances in catalysis-science & technology*, ed. T. S. R. Prasada Rao, Wiley, New York, 1985.
46 R. M. Barrer and B. M. Munday, *J. Chem. Soc. A*, 1971, 2904.
47 D. D. Eberl, *Clays Clay Miner.*, 1980, **28**, 161–172.
48 M. A. Osman, C. Moor, W. R. Caseri and U. W. Suter, *J. Colloid Interface Sci.*, 1999, **209**, 232–239.
49 K. Asselman, N. Pellens, S. Radhakrishnan, C. V. Chandran, J. A. Martens, F. Taulelle, T. Verstraelen, M. Hellström, E. Breynaert and C. E. A. Kirschhock, *Mater. Horiz.*, 2021, **8**, 2576–2583.
50 E. C. Moloy, Q. Liu and A. Navrotsky, *Microporous Mesoporous Mater.*, 2006, **88**, 283–292.
51 L. Van Tendeloo, M. Haouas, J. A. Martens, C. E. A. Kirschhock, E. Breynaert and F. Taulelle, *Faraday Discuss.*, 2015, **179**, 437–449.

52 M. Haouas, L. Lakiss, C. Martineau, J. El Fallah, V. Valtchev and F. Taulelle, *Microporous Mesoporous Mater.*, 2014, **198**, 35–44.
53 D. Vandenabeele, N. Doppelhammer, S. Radhakrishnan, C. V. Chandran, W. Wangermez, A. Rais, E. Vandeurzen, B. Jakoby, C. Kirschhock and E. Breynaert, *J. Mol. Liq.*, 2025, **417**, 126603.
54 J. Vekeman, D. Vandenabeele, N. Doppelhammer, E. Vandeurzen, E. Breynaert, C. E. A. Kirschhock and T. Verstraelen, *Chem. Mater.*, 2024, **36**, 3886–3897.
55 K. Asselman, N. Pellens, B. Thijs, N. Doppelhammer, M. Haouas, F. Taulelle, J. A. Martens, E. Breynaert and C. E. A. Kirschhock, *Chem. Mater.*, 2022, **34**, 7150–7158.
56 Y. Yokomori and S. Idaka, *Microporous Mesoporous Mater.*, 1998, **21**, 365–370.
57 N. Kamiya, K. Nishi and Y. Yokomori, *Z. Kristallogr.*, 2008, **223**, 584–590.
58 R. M. Adar, T. Markovich and D. Andelman, *J. Chem. Phys.*, 2017, **146**, 194904.
59 A. Nearchou and A. Sartbaeva, *CrystEngComm*, 2015, **17**, 2496–2503.
60 S. I. Zones, *Faraday Trans.*, 1991, **87**, 3709.
61 C. S. Cundy and P. A. Cox, *Microporous Mesoporous Mater.*, 2005, **82**, 1–78.
62 M. Houlleberghs, E. Breynaert, K. Asselman, E. Vaneeckhaute, S. Radhakrishnan, M. Anderson, F. Taulelle, M. Haouas, J. Martens and C. Kirschhock, *Microporous Mesoporous Mater.*, 2019, **274**, 379–384.
63 A. J. Mallette, G. Espindola, N. Varghese and J. D. Rimer, *Chem. Sci.*, 2024, **15**, 573–583.
64 S. Ghojavand, E. B. Clatworthy, A. Vicente, E. Dib, V. Ruaux, M. Debost, J. El Fallah and S. Mintova, *J. Colloid Interface Sci.*, 2021, **604**, 350–357.
65 M. Debost, E. B. Clatworthy, J. Grand, N. Barrier, N. Nesterenko, J.-P. Gilson, P. Boullay and S. Mintova, *Microporous Mesoporous Mater.*, 2023, **358**, 112337.
66 K. Asselman, M. Haouas, M. Houlleberghs, S. Radhakrishnan, W. Wangermez, C. E. A. Kirschhock and E. Breynaert, *Cryst. Growth Des.*, 2023, **23**, 3338–3348.
67 J. Kim and D. H. Kim, *Microporous Mesoporous Mater.*, 2018, **256**, 266–274.
68 H. Geerts-Claes, G. Vanbutsele, S. Pulinthanathu Sree, S. Radhakrishnan, C. V. Chandran, E. Breynaert, J. A. Martens and S. Smet, *Cryst. Growth Des.*, 2023, **23**, 7829–7840.
69 A. Navrotsky, O. Trofymluk and A. A. Levchenko, *Chem. Rev.*, 2009, **109**, 3885–3902.
70 R. M. Barrer and B. M. Munday, *J. Chem. Soc. A*, 1971, 2914.